Experimental and theoretical investigation of H 2 oxidation in a high temperature catalytic microreactor. Chem. Engng. Sci., 56, 1265–1273

ARTICLE *in* CHEMICAL ENGINEERING SCIENCE · FEBRUARY 2001

Impact Factor: 2.34 · DOI: 10.1016/S0009-2509(00)00348-1

PERGAMON

Chemical Engineering Science 56 (2001) 1265–1273

Chemical Engineering Science

www.elsevier.nl/locate/ces

Experimental and theoretical investigation of H_2 oxidation in a high-temperature catalytic microreactor

Götz Veser*

Chemical Reaction Engineering Group, Max-Planck-Institut für Kohlenforschung, 45470 Mülheim/Ruhr, Germany

Abstract

A sample and flexible quartz-glass-based microreactor design is presented for high-temperature catalytic gas-phase reactions. The reactor was tested with the platinum-catalysed hydrogen oxidation reaction, withstanding extremely high reaction temperatures in excess of 1000°C without any signs of degradation. Experimental results are compared to those from a previous, alternative microreactor configuration, indicating substantially reduced heat losses. No homogeneous flames or explosions are observed under any reaction conditions, indicating that homogeneous reactions can be very effectively suppressed in a microreaction channel. A theoretical analysis of the explosion limits in the homogeneous H_2/O_2-system confirms that reactors with characteristic dimensions in the sub-millimetre range become *intrinsically safe* at ambient pressure conditions. Furthermore, the analysis shows that the suppression of the explosive reaction behaviour in these microreactors can be traced to a kinetic quenching of the radical chain mechanism rather than a thermal quenching due to increased heat transfer rates.

Keywords: Microreactor design; Catalytic high-temperature reactions; Hydrogen oxidation; Explosion limits

1. Introduction

Microreactors, i.e. chemical reactors with typical dimensions (such as reactor diameter) in the sub-millimetre range, have become the topic of intense research due to the many interesting novel possibilities they offer. The potential of microreactors in the development of novel chemical process routes has been stressed repeatedly and in some cases also demonstrated in the past few years (Lerou et al., 1996; Srinivasan et al., 1997; Ehrfeld, 1997; Abraham et al., 1998; Zech & Hönicke, 1998; Hönicke, 1999). In most cases the interest in microreactors revolved around their small thermal inertia, which allows for a very direct control of the reaction temperature, their inherent safety due to the very small reactor volume and well-controllable reaction conditions, and their small overall dimensions which makes them ideal for applications where space requirements are critical (such as in mobile devices). Furthermore, the large surface-to-volume ratio typical for microreactors has been stressed often, since this results in a very short path for heat and mass transport, leading to a drastic increase in the efficiency of these mechanisms which often limit the overall reactor efficiency in conventional chemical reactors.

However, a further potential advantage of this large surface-to-volume ratio has found less attention so far: since free surfaces tend to bind radical species which are crucial as chain carriers for (particularly explosive) gas-phase reactions, the large surface-to-volume ratio could lead to an effective suppression of homogeneous gas-phase reactions. This would obviously have a couple of very interesting consequences both for applied processes as well as basic research: the suppression of (explosive) gas-phase reactions would result in an inherent safety for processes which handle potentially flammable gas mixtures, and it would also allow to study the reaction mechanisms and kinetics of high-temperature catalytic gas-phase reactions without influences by parallel homogeneous reactions, i.e. it would become possible to clearly separate homogeneous and heterogeneous contributions to the overall reaction behaviour.

We had previously reported on a simple and flexible microreactor, in which we studied the Pt-catalysed $H_2 + O_2$ reaction and could show that it is indeed possible to conduct this highly explosive reaction without the occurrence of flames or explosions in a microreactor

* Corresponding author. Tel.: +49-208-306-2455; fax: +49-208-306-2995.

E-mail address: veser@mpi-muelheim.mpg.de (Götz Veser).

0009-2509/01/$ - see front matter
PII: S0009-2509(00)00348-1

configuration (Veser, Friedrich, Freygang, & Zengerle, 1998; Veser, Friedrich, Freygang, & Zengerle, 1999). In the present contribution, we extend this study by presenting a different, even simpler microreactor which allows us to extend the temperature range for catalytic studies towards even higher temperatures ($T > 1000^{\circ}C$), and complement the experimental studies by results from a kinetic analysis of the homogeneous $H_2 + O_2$ reaction which demonstrates that by making the transition from millimetre-sized reaction channels to sub-millimetre dimensions, this normally highly explosive reaction is rendered *intrinsically* safe.

2. Experiments

2.1. Reactor design

The reactor used in the present investigation is a further development of a previous microreactor with the intent to increase the applicability of the reactor towards even higher temperatures, thus rendering the study of high-temperature catalytic reactions possible. In doing this, the major design guidelines of the previous reactor development were maintained which were: an easy handling of the reactor set-up; suitability of the microreactor for a wide range of reactions and reaction conditions; reusability of the reactor units; and easy availability or cheap fabrication techniques for the reactor parts.

While the previous reactor consisted of etched silicon chips which were housed in a sparc-eroded stainless-steel housing (Fig. 1), the new reactor design was based on commercially available quartz-glass tubes with an inner diameter of 600 μm, an outer diameter of 6 mm and a length of 20 mm (Fig. 2). The new design is thus even cheaper and simpler than the previous one. This simplicity is, however, paid off by a reduced flexibility, since the use of ready-made quartz-glass tubes limits the reactor configuration currently to straight, parallel channels. Quartz-glass was chosen as base material since macroscopic quartz-glass tubular reactors have sufficiently demonstrated their applicability to high-temperature

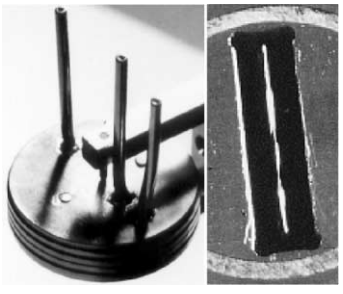

Fig. 1. Previous microreactor design: closed stainless-steel reactor housing (left) and open reactor with silicon-etched microchannels and catalytic wire (right) (adapted from Veser et al., 1998).

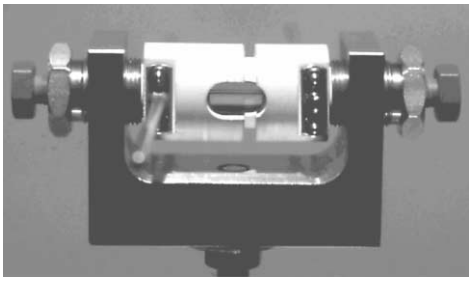

Fig. 2. Ceramic reactor housing (white) with quartz-glass tubular microreactor (visible through centre hole). Dimensions of the reactor housing are: 40 mm length, 22 mm diameter, the dimensions of the quartz-glass tube are: 20 mm length, 6 mm outer diameter, 0.6 mm inner diameter.

reactive conditions, being chemically inert in a wide of reactive environments and withstanding temperatures of up to 1250°C. Furthermore, the use of glass walls allows for a convenient optical inspection of the reaction channel during the reaction.

The quartz-glass tubes were set into a ceramic housing made from a machine-workable special ceramic which withstands temperatures of up to 1150°C after thermal annealing. Two separate feed holes on the reactor inlet side of the ceramic allow to feed two reactant streams separately and premix them by perpendicular impingement right at the microchannel entrance. This configuration assures that homogeneous reactions between the reactants in the inlet tubing can be avoided. The reaction gases are fed separately to the ceramic housing through two steel tubings which are connected to the peripherals via standard Swagelock-type connectors, thus allowing for an easy connection to standard laboratory equipment.

As in the previous reactor design, the catalyst was set into the microchannels in the form of a platinum wire. This configuration not only allows for an easy exchange and inspection of the catalyst after the reaction, but it also reduces the problems typically encountered in high-temperature environments when thin film-coated reactor walls are used (Srinivasan et al., 1997). The wire extends beyond the reactor length and is sealed through graphite sealing at both reactor ends. This allows for an easy, direct electrical contact with the catalytic wire for heating purposes during the ignition of the reaction. However, the graphite sealings in their current form only withstand a gas flow of up to ≈ 1 standard liters per minute (slpm), above which some gas leakage occurs. Here, further optimisation of the reactor design is necessary.

2.2. Experimental results

To experimentally test our new reactor configuration, we again used the $H_2 + O_2$ reaction ($H_2 + 0.5\ O_2 \rightarrow H_2O$). This reaction forms one of the most simple

combustion reactions and has been studied in much detail for many decades (Lewis & von Elbe, 1987). The reaction proceeds extremely fast, both homogeneously in the gas phase and heterogeneously catalysed by platinum. It is furthermore characterised by a particularly wide range of explosive mixtures (about 3–75 vol% in air) and very-high flame velocities and violent explosions (Lewis & von Elbe, 1987). Due to these features as well as the very simple stoichiometry of the reaction which proceeds along a single summary reaction path to yield water as the only reaction product, this reaction has been found in our previous studies to be a good candidate to test a microreactor set-up under high-temperature conditions. Beyond the pragmatic considerations for a laboratory experiment, the reaction also has some practical interest as a very efficient energy source due to its strong exothermicity ($\Delta H \approx -241$ kJ/mol). However, the wide explosion limits restrict the practical use of this reaction to special applications for which no adequate alternative fuel is available (such as in rocket propulsion), or to the use of highly diluted hydrogen/air mixtures outside the flammability region. Obviously, the reaction could be put to much wider use if a safe process could be conducted in a microreactor configuration.

In the experiment, a catalytic Pt-wire (diameter 0.15 mm, purity 99.99%) was put into the reaction channel, leaving an effective free annulus with 225 μm width for the reactive gas flow. The reaction gases H_2, O_2 and N_2 were fed through standard mass flow controllers and a thermocouple measured the temperature of the effluent gases right at the exit of the microchannel. For ignition of the reaction, synthetic air was typically introduced at a flow rate of about 0.1 slpm, and then H_2 was added to the feed gas stream. The catalytic wires were then preheated resistively in 5% H_2 in air to about 100°C before ignition of the catalytic reaction could be observed.

The steady-state temperatures of the effluent gases for various experimental conditions are shown in Figs. 3 and 4. Exit gas temperatures are shown for increasing H_2 content in 0.5 slpm synthetic air (base case, diamonds in both figures) and for reduced nitrogen dilution (0.1 slpm O_2 with 0.2 slpm N_2, Fig. 3, circles) as well as higher total flow rates (0.7 slpm synthetic air, Fig. 4, circles) The H_2 content is given as the so-called "equivalence ratio" Φ, which is defined as the actual H_2/O_2 ratio divided by the H_2/O_2 ratio at the stoichiometric point for total oxidation (which yields a common x-axis for the different experimental conditions for easier comparison).

As expected, a steep temperature rise is observed with increasing H_2 content due to increasing O_2 conversion (Veser et al., 1998). A maximum is reached near stoichiometric conditions which varies from ≈ 850°C for the base case of 0.5 slpm air to more than 1150°C for lower nitrogen dilutions, approaching the limiting

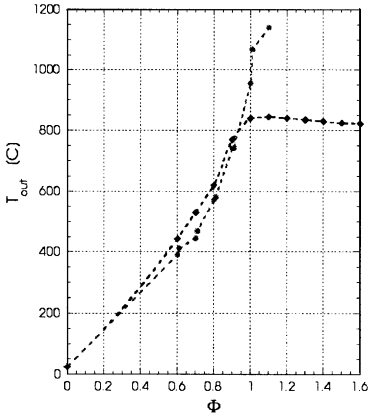

Fig. 3. Gas exit temperatures in the quartz-glass catalytic microreactor in the $H_2 + O_2$ reaction. Shown are the exit temperatures with varying H_2 content in 0.5 slpm synthetic air (diamonds) and for oxygen enriched air (0.1 slpm O_2 + 0.2 slpm N_2, circles).

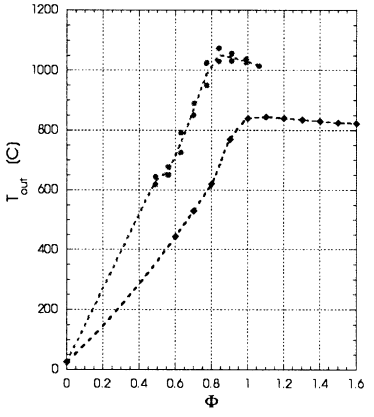

Fig. 4. Gas exit temperatures in the quartz-glass catalytic microreactor in the $H_2 + O_2$ reaction. Shown are the exit temperatures with varying H_2 content in 0.5 slpm synthetic air (diamonds) and in 0.75 slpm synthetic air (i.e., 40% higher total flow rate, circles).

temperatures of the ceramic housing. The maximum temperatures increase with decreasing nitrogen dilution (Fig. 3) as well as with increasing total flow rate (Fig. 4). The latter is indicative of substantial heat losses form the microreaction channel, since with increasing flow rate (i.e., decreasing residence time) more heat is convectively transported towards the reactor exit, thus reducing the heat losses. These heat losses can also be recognised in Fig. 3, where the reduction of N_2 dilution leads to slightly lower exit gas temperatures in the initial part of the temperature curve since the increased heat losses due to longer residence times overcompensate the large adiabatic temperature rise.

However, a direct comparison with results from our previous reactor configuration (which had been limited to temperatures below ≈ 800°C due to temperature limitations of the steel housing) show that heat losses are strongly reduced in the present reactor configuration: as

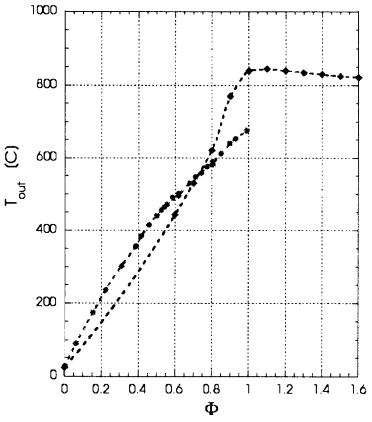

Fig. 5. Comparison between the previous silicon-based microreactor (circles) and the present glass reactor (diamonds): gas exit temperatures with increasing H_2 content in air. An air flow of 1 slpm was used in the previous reactor, while only 0.5 slpm were used in the present one.

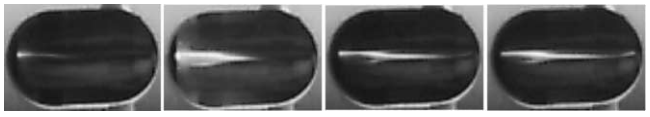

Fig. 6. Spreading of the reaction front in Pt-catalysed H_2 oxidation for a mixture of 0.1 slpm H_2 and 0.14 slpm O_2 with increasing N_2 flow (from left to right: 0.15, 0.25, 0.35, 0.45 slpm). Gas flow is from left to right.

shown in Fig. 5, maximum temperature is increased by about 200°C in the new reactor despite the substantially lower flow rates (0.5 slpm air vs. 1 slpm in the old reactor). Extrapolating from the results in Fig. 4, maximum temperatures around 1300°C should be reachable in the new reactor configuration if the sealing is improved to withstand the gas flow corresponding to 1.0 slpm air.

A visual inspection of the reaction channel under steady-state conditions demonstrates that the exit gas temperatures are well below the actual reaction temperatures in the microchannel. As shown in Fig. 6, a very bright, white-glowing hot spot develops in the reactor near the reactor entrance, indicating that the reaction proceeds catalytically so fast that for low flow rates all hydrogen is consumed over the first few mm of the catalytic wire already. Correspondingly, the back part of the reactor is dark in the picture, indicating that massive heat losses due to the large reactor surface area lead to a rapid cooling of the reaction gases. From the almost white colour of the glowing Pt wire the local reaction temperature can be estimated to be well in excess 1200°C.

As further apparent from the sequence in Fig. 6, the hot spot can be moved along the reactor axis by increasing the total flow rate, for example by increasing the N_2 flow. Residence times become so short that the reaction front is eventually smeared out over the whole reactor length. It seems remarkable that residence times as short as 50 μs could be reached in these simple experiments. Obviously, through minor modifications of the reactor channel diameter and/or the catalyst wire thickness this number could be further reduced, so that it might become possible to study the spatial reaction progress in a typical high-temperature catalytic reaction by spreading out the reaction along a microreaction channel. This indicates again some of the great potential microreactors hold as valuable tools for the study of the mechanisms and kinetics of catalytic reactions as well as the general behaviour of catalytic reactors.

Overall, the experiments reveal a reaction behaviour which shows no qualitative differences between the two microreactor configurations, and no obvious deviation from the expected behaviour in a conventional "macroscopic" catalytic fixed-bed reactor — except for one fundamental difference: under all reaction conditions, even at temperatures in excess of 1000°C and at stoichiometric compositions for the oxidation reaction, no open flames or explosions were ever observed. Obviously, this is *completely* different from the reaction behaviour in conventional reactors, where these experiments would be effectively impossible since the reactor would blow up at all experimental conditions shown above.

Thus, it seems that the effective suppression of homogeneous reactions that we had observed in the previous reactor configuration was sustained in new reactor design. It seems therefore, that this suppression is rather independent of the channel material and details of the particular reactor configuration. Furthermore, the fact that this suppression of an explosive behaviour could be achieved even with the substantially reduced heat losses in the new reactor configuration seems to indicate, that a thermal quenching of the homogeneous reaction is not the only factor (or may be not even a factor at all) determining this behaviour. To address this point, we undertook a theoretical analysis of the reaction kinetics, a brief summary of which will be given in the next section.

3. Theoretical investigation

The above experiments demonstrated that the explosive behaviour of the homogeneous reaction can be effectively suppressed in our microreactor configurations. However, the experimental results do not allow to distinguish between the quenching of a thermal explosion of the reaction because of high heat transfer rates (i.e., heat losses to the environment), and the quenching of kinetic explosion based on the radical scavenging effect of the reactor walls. While in a *kinetic explosion* the chain branching mechanism leads to the creation of two (or more) highly reactive gas-phase radicals from one radical, in a *thermal explosion* the heat evolved in the

exothermal (combustion) reaction leads to an self-acceleration of the reaction through the temperature-dependent rate coefficients. Both mechanisms rely on a positive feedback in the reaction mechanism, either thermally or by way of reactant concentrations. Experimentally, these mechanisms are usually very difficult (if not impossible) to distinguish, since typical radical chain reactions are sufficiently exothermic to lead to a rapid increase in reaction temperature once a homogeneous flame occurs, and an increase in reaction temperature is typically accompanied by a strong increase in radical concentrations.

It seems to be rather common knowledge that H_2/O_2 mixtures display a quenching distance of about 1 mm (see for example, Williams, 1984; Lewis & von Elbe, 1987). However, since this critical value is exactly in the order of magnitude of our reactor dimensions and since no clear derivation of this value as well as a critical discussion of thermal vs. kinetic explosion mechanism seemed to be available in the published literature, we decided to conduct a detailed kinetic analysis of the reaction mechanism to answer these questions, which are obviously crucial to a true understanding of our experimental results. Due to space limitations, only a brief summary of the results can be given here and the reader is referred to a more comprehensive upcoming publication for more details (Veser, 2001).

3.1. Reaction mechanism

Typical combustion processes such as the H_2 oxidation are based on radical chain mechanisms (Laidler, 1987; Williams, 1984). For the H_2/O_2 system, a complete mechanism comprises more than 40 elementary reaction steps (Baldwin & Walker, 1972). For the present investigation, however, simplified reaction mechanisms following Lewis and von Elbe (1987) and Scott (1995) were used, which have been shown to grasp the essential features of the reaction mechanism well.

In such radical chain mechanisms, four different basic reaction steps are usually distinguished: The reaction is started by *chain initiation steps*, in which reactive radicals are formed from stable molecules. These radicals are the true "carriers" of the reaction and can propagate the reaction either in a controlled way in *chain propagation steps*, in which they react with molecules to give one new radical, or in *chain branching reactions*, in which they react with a molecule to give *two* (or more) new radical species. It is this latter type of reaction that is responsible for kinetic explosions, since the formation of two highly reactive radicals form one yields a positive feedback mechanism in the reaction scheme which will lead to a self-acceleration of the reaction unless it is countered by some very strong "limiting" mechanism. This can be provided by the *chain termination steps*, in which radicals react to more stable molecules, either in the gas phase or at the reactor walls. This wall-induced chain termination could lead to a suppression of chain branching and thus explosive behaviour in a microreactor.

3.2. Explosion limits

The curves which delimit explosive from well-controlled reaction behaviour are usually referred to as "explosion limits" and plotted in p, T-explosion diagrams. For the H_2/O_2 reaction, this explosion limit is characterised by two turning points which separate the curve into three explosion limits, of which the first one extends from very low pressures up to the first turning point, the second one connects the two turning points and lies at intermediate temperatures and pressures, and the third one completes the curve from the second turning point towards higher pressures (for a detailed description, see for example, Williams, 1984; Lewis & von Elbe, 1987).

Even though the exact quantitative determination of the explosion limits requires rather detailed simulations with the full reaction mechanism, the processes that lead to the occurrence of the observed explosion limits are qualitatively easy to understand. At very low pressures (below about 5 mbar), the reaction remains virtually unreactive since the mean free path of the molecules is large in comparison to the reactor dimensions. Thus, a reactive collision between two molecules is unlikely and the few reactive species that are formed quickly react to stable molecules at the reactor walls. With increasing pressure in the reaction vessel, intermolecular collisions become more and more probable as the mean free path decreases, until the *first explosion limit* is crossed and reactive events outnumber wall collisions. Due to the above-mentioned positive feedback in the reaction mechanism an explosive self-acceleration occurs. Since this explosion limit is determined by the competition between wall reactions and intermolecular reactions, it is dependent on the diffusion of the reactive particles to the reactor walls and can thus be expected to be strongly dependent on the dimensions of the reaction vessel.

Upon a further increase of the pressure, the reaction remains explosive until the *second explosion limit* is reached and the reaction suddenly falls back to a slow, controlled reaction state due to the increasing contribution of trimolecular reaction events, which constitute chain propagation rather than chain branching steps and thus counter the explosive self-acceleration.

At even higher pressures, the reaction shows again a sudden transition to an explosive behaviour. The explanation for this *third explosion limit* is less straightforward, since both a thermal as well as kinetic effect can lead to explosive behaviour at this point. This will be discussed further in Section 3.2.3.

The exact location of the explosion limits thus depends on various factors such as the size of the reaction vessel,

the surface-to-volume ratio, and the initial reactant concentrations (including inert components, such as N_2). Only a very brief outline of the determination of the explosion limits can be given here due to space constraints. The equations were based on two major simplifications: a closed, spherical reactor geometry was assumed and the above-mentioned simplified reaction schemes were used. It can be shown, however, that neither of these two assumptions has a strong influence on the results of the derivation (Veser, 2001).

Based on the distinction of three fundamentally different types of reaction steps in the H_2/O_2 reaction system, we separate the reaction into *chain initiation steps*, in which radicals (or chain carriers) are formed at a rate θ, *chain branching steps*, in which the concentration of the chain carriers n increases at a rate $f[n]$, and *chain termination steps*, in which the concentration of chain carriers is reduced either by gas-phase reactions at a rate $g[n]$ or by reactions at the reactor wall at a rate $\gamma[n]$.

This results in the following simple rate law for the chain carriers n (Baldwin & Walker, 1972);

$$\frac{\mathrm{d}[n]}{\mathrm{d}t} = \theta + f[n] - g[n] - \gamma[n]$$

$$= \theta + \phi[n], \tag{1}$$

where $\phi = f - g - \gamma$ denotes the net *branching factor*.

For fixed initial conditions (composition, T, p) and assuming negligible conversion, θ and ϕ are constant and the integration of Eq. (1) with the initial condition $[n]_{t=0} = 0$ yields

$$[n] = \theta t \qquad \text{for } \phi = 0, \tag{2}$$

$$[n] = \frac{\theta}{\phi}(\exp(\phi t) - 1) \qquad \text{for } \phi \neq 0. \tag{3}$$

While for $\phi < 0$, the latter expression results in a constant expression ($-\theta/\phi$, corresponding to a slow, controlled reaction), for $\phi > 0$, the exponential term will yield an exponential growth of [H] and thus an explosive course of the reaction. The interesting limiting case is thus $\phi = 0$, which denotes the explosion limit.

Eq. (1) must usually be solved for all chain carriers and the simultaneous solution of the resulting set of coupled equations yields the explosion limit. However, for the H_2/O_2 system it is known that $H\cdot$ radicals are substantially less reactive than $O\cdot$ and $OH\cdot$, and the latter can therefore be assumed to be at quasi-steady state. Thus, the analysis of Eq. (1) for $H\cdot$ radicals alone yields the explosion limits for the current reaction system. In the following, the results for the three explosion limits will be discussed only for stoichiometric mixture of H_2 and O_2, although the main results hold similarly for other ratios and a wide range of N_2 dilutions.

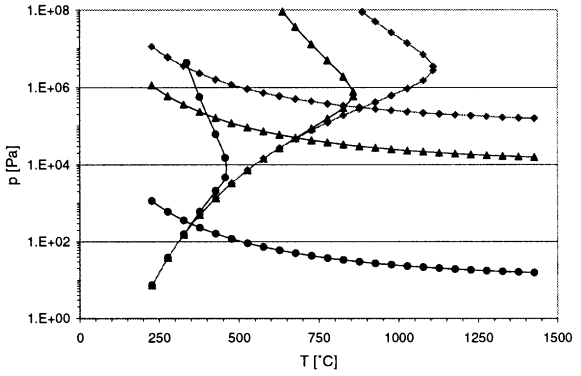

Fig. 7. The three kinetic explosion limits for a stoichiometric H_2/O_2 mixture and three different reactor diameters: $d = 1$ splm (circles), $d = 1$ mm (triangles) and $d = 100$ μm (diamonds). The explosive regime is the upper right area that is delimited towards lower pressures and temperatures by the crossing of any of the three limit curves.

The results of the derivation of the explosion limits are summarised in Fig. 7, which depicts the explosion limits a stoichiometric H_2/O_2 mixture for three different reactor diameters of 1 m, 1 mm and 100 μm.

The three explosion limits, which bound the range of explosive reaction behaviour towards lower temperatures and pressures, and their dependence on reactor dimensions will be discussed briefly in the following.

3.2.1. First explosion limit

From the above discussion of the ignition limits it can already be expected that a strong dependence of the first ignition limit on the reactor dimensions should be found. Since the ignition limit is determined by the interplay between the (explosive) gas-phase reaction and the quenching influence of the reactor walls, smaller reactor dimensions facilitate the diffusion of the reactants to the reactor walls and thus increase the explosion limit.

This is confirmed by our analysis as seen in Fig. 7. Clearly, the first explosion limit (which is given by the rather flat horizontal line) is strongly dependent on the reactor dimensions, with a drastic increase in the explosion limit with decreasing reactor diameter.

Despite the qualitatively obvious influence of the longer diffusion path on the ignition process, it seems surprising to find such a strong dependence. The mean free path for $H^{\cdot}$ radicals is about 400 nm at atmospheric pressure and $T = 800^{\circ}$C, which is several orders of magnitude smaller than any reactor dimension considered here. Thus, only a small number of free radicals should be able to reach the wall without any prior intermolecular collisions. Clearly, the extreme sensitivity of the reaction to the radical concentration near the ignition limit leads to a very strong effect of this small perturbation.

3.2.2. Second explosion limit

No strong influence of reactor dimensions on the position of the position of the second explosion limit is expected, since this limit is determined by the interplay between different gas-phase reaction pathways. Indeed, virtually no dependence of the second explosion limit on reactor dimensions is observed (except for the transition region close to the third explosion limit). As already shown by Lewis and von Elbe (1987), the limiting cases of infinitely large to infinitely small reactor dimensions differ only by a factor of 2/3, which is obviously negligible in the logarithmic scale of Fig. 7.

3.2.3. Third explosion limit

The third explosion limit constitutes the most interesting case. First of all, it is the third explosion limit which is normally responsible for the occurrence of an explosion under ambient pressure conditions. Thus, this limit has a particular importance for very practical reasons. Furthermore, both a kinetic explosion as well as a thermal explosion are possible mechanisms under these comparatively high pressure conditions (compared to the other two explosion limits). At this explosion limit, particularly wall reactions of H_2O_2 species are known to play an important role for the renewed onset of explosive behaviour. Correspondingly, a strong dependence of the third explosion limit on reactor dimensions is observed again in our analysis (Fig. 7). However, unlike for the first explosion limit where decreasing reactor dimensions essentially lead to a vertical parallel-shift of the curve, the third explosion limit is shifted substantially both towards higher pressures and higher temperatures, and the slope of the explosion limit is flattening in the course of this shift. While the influence of the reaction diameter on the first explosion limit was mainly based on the dependence of the diffusion process, i.e. on the length of the diffusion path, the third explosion limit is now determined by the detailed interplay of the elementary reaction steps and thus shows a much more complex dependence on reactor dimensions.

In contrast to this "kinetic explosion", the thermal explosion mechanism relies on the increased heat production caused by the increasing reaction rate with higher pressures. This heat production leads to a positive feed back due to the Arrhenius-type temperature dependence of the reaction rate and thus a self-acceleration of the reaction rate (i.e. an explosion) occurs. The determination of the thermal explosion limit is, therefore, be based on an energy balance of the system, balancing the chemical heat production with the heat losses from the reactor. The heat transfer coefficient for the microreactor was, therefore, calculated based on standard heat transfer correlations (VDI, 1991), using typical values (wall thickness, wall materials) from our experimental microreactor set-up.

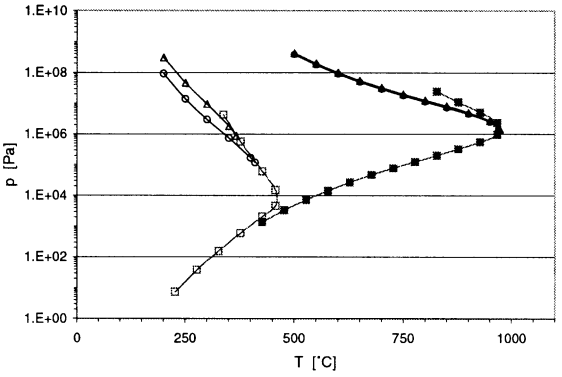

Fig. 8. Kinetic explosion limits (squares) and thermal explosion limits (calculated for $T_{wall} = T_{room}$ (circles) and $T_{wall} = T_{reaction}$ (triangles)) for a reactor with 300 μm (filled symbols) and 1 m diameter (open symbols).

Fig. 8 shows a comparison between the calculated thermal and kinetic explosion limits for a "macroscopic" reactor ($d = 1$ m) and a microreactor ($d = 300$ μm). Since the reactor wall temperature is necessary for the heat loss calculations, two limiting cases for the thermal explosion limit are shown, with the reactor walls assuming the reaction temperature (triangles) and the reactor walls remaining at room temperature (circles). As apparent from the graph, the exact wall temperature has a noticeable but not decisive influence on the position of the third limit for a macroscopic reactor, while the two curves becomes essentially indistinguishable for a microreactor with reactor dimensions in the submillimetre range.

One can furthermore see, that the thermal explosion limit lies below the kinetic explosion limit for all conditions, in agreement with the somewhat simplifying denotion of this explosion limit as "thermal explosion" in many textbooks. Interestingly, however, the "branching" of the thermal explosion limit from the kinetic explosion limit occurs for the macroscopic reactor right around $p = 10^5$ Pa, i.e. around ambient pressure. Clearly, in a typical ambient pressure experiment a distinction between these two explosion limits will be impossible. Due to the higher heat losses from the small microchannels, this difference between the thermal and the kinetic explosion limit becomes more pronounced in a microreactor.

3.3. Discussion: ignition in microchannels

The analysis of the reaction mechanism at the explosion limits thus confirmed our experimental findings that an effective suppression of explosive homogeneous gas-phase reactions can indeed be expected in a sufficiently small microreactor. Beyond this confirmation, the analysis further explains this suppression not simply by

a "thermal quenching" of the homogeneous reaction due to the heat losses from a microreactor but rather by a "radical quenching", i.e. a kinetic effect. This is an important distinction since it indicates that a microreactor will remain a safe reactor configuration even when heat losses from the reaction channel are further reduced by an appropriate reactor design.

The drastic qualitative changes in going from a conventional (macroscopic) reactor to a microreactor become particularly apparent when looking at increasing reaction temperatures at ambient pressure conditions (i.e $p = 10^5$ Pa in Fig. 7): for a conventional reactor with 1 m diameter, explosive behaviour sets in upon crossing the third explosion limit around $T = 420°C$. Decreasing the reactor diameter to 1 mm, explosion occurs at substantially higher temperatures ($T \approx 750°C$) by crossing the *second* explosion limit. If the reactor diameter is now reduced by another order of magnitude from 1 mm to 100 μm, the explosive reaction regime gets pushed further towards higher pressures and temperatures, so that even the first ignition limit is raised above ambient pressure conditions *and explosive behaviour can generally be excluded, i.e. the reaction becomes inherently safe.*

It should also be mentioned that this result was qualitatively confirmed by an experimental observation during the test phase of our reactor configuration: according to the theoretical analysis, the critical transition to an inherently safe reaction behaviour occurs in the transition from a characteristic reactor dimension in the order of 1 mm to 100 μm. In agreement with that, we observed during our experiments that a premixed H_2/O_2 mixture ignited homogeneously in a feed tube with 2 mm inner diameter, while no ignition was ever observed when the gases were fed separately to our microreactors with their characteristic dimensions of ≈ 200 μm.

4. Summary

The Pt-catalysed H_2 oxidation was investigated in simple and flexible microreactors configurations as a test case for the applicability of microreactor concepts for high-temperature catalytic gas-phase reactions. A novel quartz-glass-based reactor configuration was presented and compared with results from a previous, silicon-based reactor. Both configurations proved to be simple, flexible and well suited to high-temperature reactive atmospheres. While some sealing problems of the quartz-glass reactor at higher flow rates still remain at this point, this reactor set-up is an extremely simple and cheap microreactor configuration which offers the additional advantage of allowing a visual inspection of the catalytic reaction channel under reaction conditions.

An effective suppressions of homogeneous flames and explosions was found in both microreactors over a wide range of feed and reaction conditions. A theoretical analysis of the explosion limits in the homogeneous H_2/O_2-system confirmed that the suppression of the explosive reaction behaviour in these microreactors can indeed be traced to a kinetic quenching of the radical chain mechanism rather than a thermal quenching due to increased heat transfer rates. It could be shown that microreactors with characteristic dimensions below 1 mm become *intrinsically* safe for this reaction system at ambient pressure conditions. While the derivation strictly only applies to the H_2/O_2-reaction, similar effects can be expected for other radical chain reactions, although the full extent of the wall quenching has to be tested individually for each reaction system.

Overall, the results of this study indicate the great potential of catalytic microreactors, particularly as laboratory tools for the exploration of new reaction pathways in hitherto "forbidden" parameter regions, but also for the practical application in highly explosive reaction systems.

Acknowledgements

The author gratefully acknowledges financial assistance by the "Deutsche Forschungsgemeinschaft" (DFG) as well as the skillful assistance by Thorsten Schmitt.

References

Abraham, M., Ehrfeld, W., Hessel, V., Kamper, K. P., Lacher, M., & Picard, A. (1998). Microsystem technology: Between research and industrial application. *Microelectronic Engineering*, *41/42*, 47–52.

Baldwin, R. R., & Walker, R. W. (1972). Chain branching reactions: The hydrogen–oxygen reaction. *Essays in Chemistry*, *3*, 1–37.

Ehrfeld, W. (1997). (Ed.). *Microreaction technology*. Berlin: Springer.

Hönicke, D. (1999). Microchemical reactors for heterogeneously catalysed reactions. In G. C. Froment, & K. C. Waugh (Eds.), Reaction kinetics and the development of catalytic processes. Amsterdam: Elsevier.

Laidler, K. J. (1987). *Chemical kinetics*. New York: Harper Collins.

Lerou, J. J., Harold, M. P., Ryley, J., Ashmead, T. C., O'Brien, M., Johnson, J., Perrotto, C. T., Blaisdell, T. A., Rensi, T. A., & Nyqvist, J. (1996). Microfabricated minichemical systems: Technical feasability. In W. Ehrfeld (Ed.), *Microsystem technology for chemical and biological microreactors*. DECHEMA Monographs, vol. 132 (pp. 51–70). Weinheim: VCH.

Lewis, B., & von Elbe, G. (1987). *Combustion and flames and explosions of gases*. New York: Academic Press.

Scott, S. K. (1995). *Oscillations, waves and chemical kinetics*. Oxford: Oxford Science Publications.

Srinivasan, R., Hsing, I. -M., Berger, P. E., Firebaugh, S., Jensen, K. F., & Schmidt, M. A. (1997). Micromachined chemical reactors for heterogeneous catalytic partial oxidation reactions. *A.I.Ch.E. Journal*, *43*, 3059–3069.

Verein Deutscher Ingenieure (VDI), (1991). *VDI-Wärmeatlas*. Düsseldorf: VDI-Verlag.

Veser, G. (2001). Ignition in microreaction channels: A theoretical investigation of the H_2 oxidation reaction, in preparation.

Veser, G., Friedrich, G., Freygang, M., & Zengerle, R. (1998). A simple and flexible microreactor for investigations of heterogeneous catalytic gas phase reactions. *ASMEDSC*, *66*, 199–206.

Veser, G., Friedrich, G., Freygang, M., & Zengerle, R. (1999). A simple and flexible microreactor for investigations of heterogeneous catalytic gas phase reactions. In G. F. Froment, & K. C. Waugh (Eds.), *Reaction kinetics and the development of catalytic processes*. Amsterdam: Elsevier.

Williams, F. A. (1984). *Combustion theory*. Menlo Park, CA: Benjamin/Cummings.

Zech, T., & Hönicke, D. (1998). Microreaction technology: Potentials and technical feasability. *Erdöl, Erdgas, Kohle*, *114*, 578–581.